



**HAL**  
open science

# Honey Maps the Pb Fallout from the 2019 Fire at Notre-Dame Cathedral, Paris: A Geochemical Perspective

Kate E Smith, Dominique Weis, Catherine Chauvel, Sibyle Moulin

► **To cite this version:**

Kate E Smith, Dominique Weis, Catherine Chauvel, Sibyle Moulin. Honey Maps the Pb Fallout from the 2019 Fire at Notre-Dame Cathedral, Paris: A Geochemical Perspective. *Environmental Science and Technology Letters*, 2020, 7, pp.753 - 759. 10.1021/acs.estlett.0c00485 . hal-02990437

**HAL Id: hal-02990437**

**<https://hal.science/hal-02990437>**

Submitted on 16 Nov 2020

**HAL** is a multi-disciplinary open access archive for the deposit and dissemination of scientific research documents, whether they are published or not. The documents may come from teaching and research institutions in France or abroad, or from public or private research centers.

L'archive ouverte pluridisciplinaire **HAL**, est destinée au dépôt et à la diffusion de documents scientifiques de niveau recherche, publiés ou non, émanant des établissements d'enseignement et de recherche français ou étrangers, des laboratoires publics ou privés.

# Honey maps the Pb fallout from the 2019 fire at Notre-Dame Cathedral, Paris: a geochemical perspective

Kate E. Smith<sup>\*,1</sup>, Dominique Weis<sup>\*,1</sup>, Catherine Chauvel<sup>2</sup>, Sibyle Moulin<sup>3</sup>

<sup>1</sup> Pacific Centre for Isotopic and Geochemical Research, Department of Earth, Ocean and Atmospheric Sciences, University of British Columbia, 2020-2207 Main Mall Vancouver, BC, V6T 1Z4, Canada.

<sup>2</sup> Université de Paris, Institut de physique du globe de Paris, CNRS, F-75005 Paris, France.

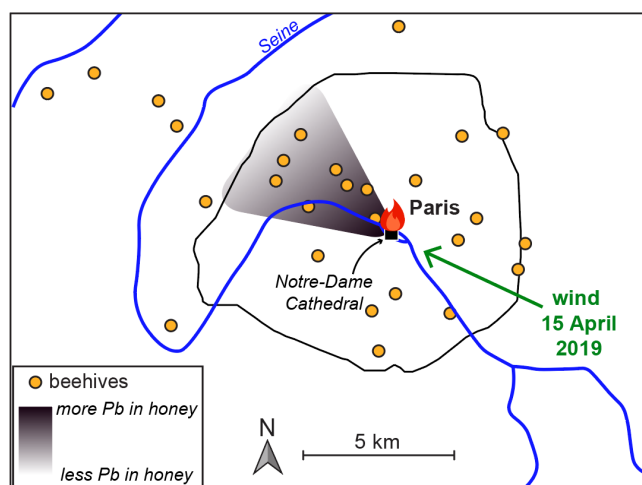
<sup>3</sup> Beeopic, Route de Vauhallan, 91400 Saclay, France.

\*Correspondence to: [katesmith@eoas.ubc.ca](mailto:katesmith@eoas.ubc.ca), [dweis@eoas.ubc.ca](mailto:dweis@eoas.ubc.ca)

## ABSTRACT

The fire at Notre-Dame cathedral, Paris, in April 2019 was an acute pollution event, releasing lead- (Pb-) rich dust into the city. To assess Pb distribution, honey samples (n = 36) were collected (in July 2019) from hives throughout the Île-de-France following the fire and were analyzed for a suite of metal concentrations and Pb isotopic compositions. Honey from hives downwind of the fire has elevated Pb concentrations (0.023 µg/g Pb, geometric mean) compared to other honey from central Paris (0.008 µg/g), pre-fire Paris (0.009 µg/g), and the Rhône-Alpes region (0.004 µg/g). The Pb isotopic range for all analyzed honey (Paris and Rhône-Alpes, 1.144-1.179 <sup>206</sup>Pb/<sup>207</sup>Pb, 2.079-2.125 <sup>208</sup>Pb/<sup>206</sup>Pb) falls within the modern Pb isotopic range for French aerosols and sediments, signifying that the fire did not perturb the isotopic composition of Parisian honey. The variations in downwind Pb concentrations demonstrate the utility of honey as a biomonitor after an acute pollution event while the isotope results are supported by the construction history of Notre Dame cathedral and historical record of Pb ores used throughout France.

## TOC ART

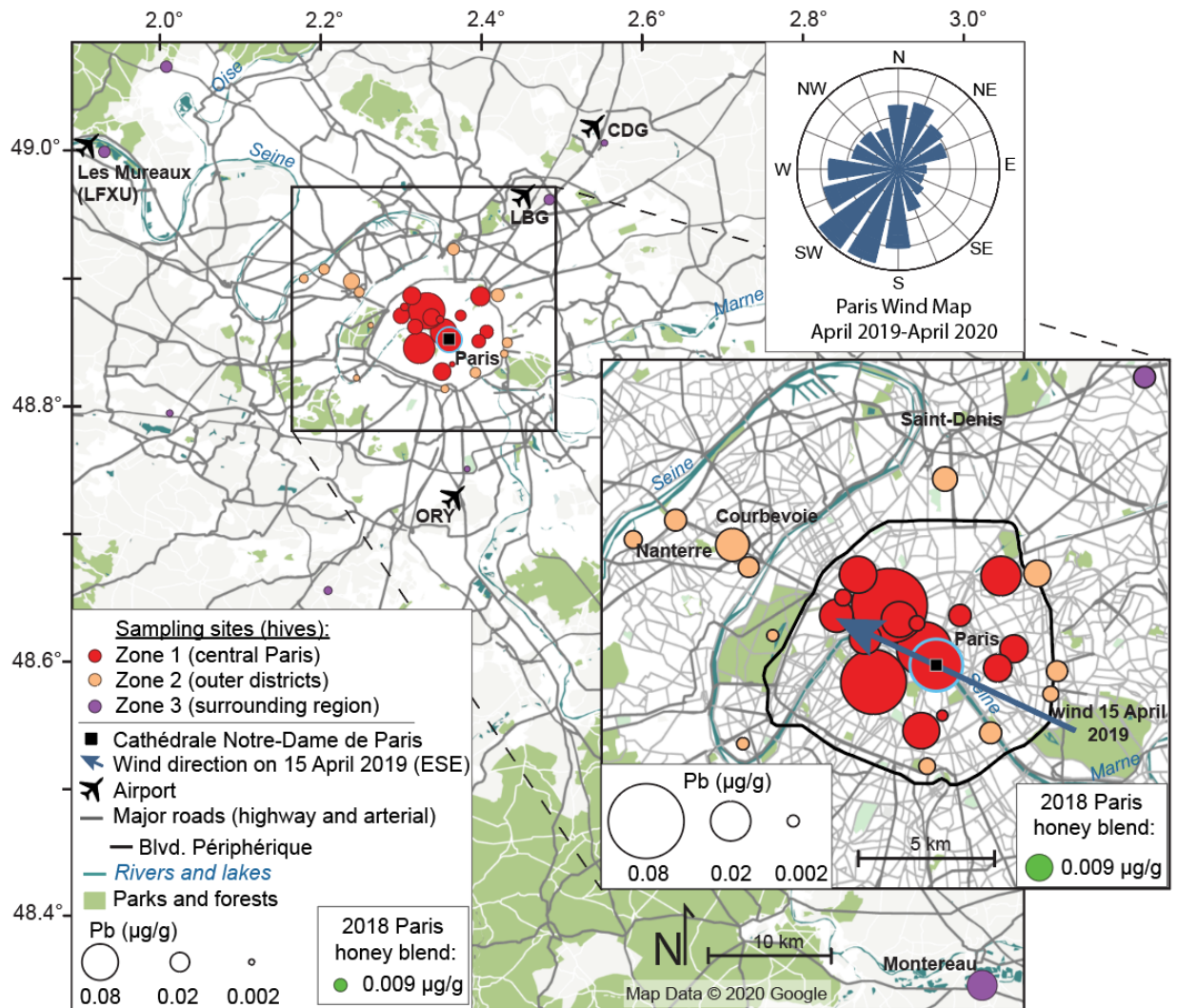


## INTRODUCTION

Lead (Pb) has served many uses since its earliest production in antiquity (~7000 BCE), including as a convenient building material because it resists corrosion, is plentiful, and is

31 quite malleable.<sup>1</sup> Uses of Pb in Paris historically include roofing, water pipes, sheathing for  
32 copper cables, paint additives, leaded gasoline, and batteries.<sup>2</sup> A Pb roof was installed on  
33 Notre-Dame de Paris cathedral at the end of the twelfth century and Pb gutters followed  
34 soon after. The Pb roof underwent various repairs in the eighteenth century, and the old  
35 spire was removed in 1786, to be replaced with a new, Pb-covered, oak spire in 1859-60.<sup>3</sup>

36 On 15 April 2019, a fire started in the attic of Notre-Dame, and eventually engulfed  
37 the spire and parts of the roof, which consist of several hundred tonnes (Mg) of lead. While  
38 most of the lead simply melted (elemental Pb melts at 327.5°C and vaporizes at 1700 °C),  
39 post-fire palaeothermometry investigations of the burned oak confirmed that parts of the  
40 fire exceeded 600 °C (with highest temperatures reaching 1200 °C), which was more than  
41 hot enough to aerosolize various Pb oxides.<sup>4</sup> As a result, an estimated 180 tonnes of Pb  
42 remain unaccounted for amongst the melted rubble.<sup>5</sup> While a south-westerly wind is  
43 common during most of the year in the Île-de-France<sup>6</sup>, the wind was blowing from the east-  
44 southeast on the night of the fire, pushing the plume of smoke, ash, and dust (containing Pb  
45 oxide aerosols) westward (Fig. 1).



46

47 **Fig. 1.** Map of Paris and surroundings showing the locations of hives where honey was  
 48 collected in 2019, after the fire at Notre-Dame de Paris. Symbol size denotes Pb  
 49 concentration measured in the honey (note different scales for the main map and inset).  
 50 Symbol colors denote three sampling zones: Zone 1 is central Paris, within Blvd.  
 51 Périphérique; Zone 2, on or just beyond Blvd. Périphérique; Zone 3, surrounding regions.  
 52 The red symbol with blue outline denotes honey collected from a hive at Notre-Dame (on  
 53 the sacristy rooftop, immediately south of the main cathedral). Lead concentration  
 54 (depicted by symbol size) for the 2018 Paris honey blend, from several hives within Paris<sup>7</sup>,  
 55 is included in the legend. Airport codes are CDG = Charles de Gaulle, LBG = Le Bourget, ORY =  
 56 Paris-Orly, LFXU = Les Mureaux airfield. The large blue arrow indicates the wind direction on  
 57 the night of the fire, and the wind rose represents composite wind data for one year in  
 58 Paris, April 2019-April 2020 (station location: 48.85°N 2.35°E, compiled from meteoblue<sup>6</sup>).  
 59

60 Honey (and other hive products) from *A. mellifera* (European honey bee) are used  
 61 for environmental monitoring of numerous analytes, including organic residues (e.g.  
 62 pharmaceuticals from veterinary hive treatments and pesticides in agricultural settings)<sup>e.g.,8-</sup>

63 <sup>10</sup> and metals, particularly in urban settings or near a major point-source of metal  
64 pollution.<sup>11,12</sup> Honey bees actively interact with multiple environmental domains (air, water,  
65 soil, vegetation) and passively collect dust while they forage (2-3 km radius), so the  
66 elemental composition of their honey (and bee tissue and other hive products) reflects  
67 metal distributions in the environment (although at relatively lower concentrations in the  
68 honey compared to other hive matrices).<sup>13,14</sup> Since bees unavoidably collect dust and  
69 airborne particles during foraging,<sup>15,16</sup> there is indeed a correlation between these  
70 environmental domains, such that areas of high Pb concentrations in dust and topsoil are a  
71 predictor of elevated levels of Pb in honey.<sup>12</sup>

72           Lead isotopic compositions of honey provide additional information by permitting  
73 assessments of potential sources of Pb in the environment surrounding the hive.<sup>11,12,14</sup> All  
74 Pb sources and sinks are composed of various relative abundances of four stable isotopes:  
75 <sup>204</sup>Pb, <sup>206</sup>Pb, <sup>207</sup>Pb, and <sup>208</sup>Pb. The Pb isotopic composition of a material is a function of the  
76 abundance of primordial (non-radiogenic) <sup>204</sup>Pb, initial amounts of the parent isotopes (<sup>238</sup>U,  
77 <sup>235</sup>U, <sup>230</sup>Th, which decay to radiogenic <sup>206</sup>Pb, <sup>207</sup>Pb, <sup>208</sup>Pb, respectively), and age of the  
78 geologic material that contained the Pb. As a result, the isotopic composition of a material  
79 can offer insight into Pb source(s), a hypothesis used extensively in environmental  
80 assessments.<sup>e.g.,17,18</sup> Lead source apportionment applications are particularly important for  
81 environmental monitoring since Pb is a toxic metal, and not easily removed or remediated  
82 once released into the environment, prompting great concern for public health due to its  
83 neurotoxic effects, especially for children.<sup>19</sup>

84           In this study, we present geochemical data for thirty-six Parisian honey samples  
85 collected during the summer following the Notre-Dame fire (Fig. 1). We report Pb isotopic  
86 compositions and concentrations for 22 elements (Mg, Al, Ti, V, Cr, Mn, Fe, Co, Ni, Cu, Zn,

87 Ga, As, Rb, Sr, Zr, Mo, Cd, Sn, Sb, Ba, Pb, Table S1), which were selected to include a mixture  
88 of major and trace elements originating from either lithogenic or anthropogenic sources (or  
89 both). For context, we also completed analyses of a Parisian honey blend from 2018 and  
90 twelve Alpine honey samples collected in 2017 from the Auvergne-Rhône-Alpes region,  
91 including samples from Grenoble, France (Fig. S1). This data was used to compare metal  
92 concentrations and geospatial trends to those of other environmental proxies (e.g.,  
93 aerosols) in Paris, as well as honey from another French city (Grenoble), and to assess the  
94 impact that the fire at Notre-Dame de Paris in April 2019 may have had on Pb in Parisian  
95 honey in terms of concentration and isotopic composition. As honey is becoming a more  
96 established urban biomonitor of Pb distribution, the Notre-Dame fire provides a unique  
97 opportunity to assess the efficacy of honey as an environmental monitoring tool after an  
98 acute Pb pollution event, rather than gradual (e.g., global use of leaded gasoline throughout  
99 the twentieth century caused pervasive, chronic Pb pollution). Furthermore, this is the first  
100 application of Pb isotope analysis of honey in a megacity with long (millennia-scale) history  
101 of Pb use.

102

## 103 **MATERIALS AND METHODS**

104 Beeopic is a Parisian apiary company that manages approximately 350 hives  
105 throughout the Paris conurbation. Beeopic provided honey from 36 sites, collected in July  
106 2019 (Fig. 1). The honey was sampled directly from the hive: fresh, capped honey was  
107 collected from the honey super box into pre-cleaned (acid-leached), polyethylene vials (i.e.  
108 following the sampling methods of Smith et al.<sup>11</sup> and Smith and Weis<sup>14</sup>). Sampling in July  
109 following the fire is reasonable considering several factors: the tendency of Pb to linger  
110 (especially bound in topsoil) once deposited in the environment<sup>20,21</sup>, the kinetics of honey

111 production (i.e., worker bee life cycles, inter-seasonal reproducibility of metals<sup>14</sup>), and a  
112 required contribution of ~100,000 foraging flights to produce 1 kg of honey, ensuring a  
113 natural threshold of homogeneity in the honey.<sup>22</sup> A Parisian honey was purchased in 2018  
114 from the company Le Miel de Paris, that produces blended honey from hives located  
115 throughout central Paris<sup>7</sup> and represents a sample of Parisian honey from before the Notre-  
116 Dame de Paris fire in April 2019. Honey from the Rhône-Alpes region was provided by  
117 citizens with backyard beehives (n = 9) or purchased as commercially available honey (n =  
118 3).

119 All samples were analyzed for metal concentrations and Pb isotopic compositions  
120 (Table S1) at the Pacific Centre for Isotopic and Geochemical Research at the University of  
121 British Columbia, Canada. All work was performed in a clean laboratory setting, following  
122 the procedures and quality control practices of Smith et al.<sup>11</sup>: metal and Pb isotopic analyses  
123 were completed on HNO<sub>3</sub>-digested honey via inductively-coupled plasma mass  
124 spectrometry (ICPMS, Agilent 7700x, Agilent Technologies, Santa Clara, CA, USA) and high-  
125 resolution (HR-)ICPMS (Nu AttoM, Nu Instruments Ltd., Wrexham, UK), respectively. Each  
126 digestion and analytical batch contained standard reference material (NIST 1568b),  
127 procedural blanks, and procedural and analytical duplicates (Table S2).

## 129 **RESULTS AND DISCUSSION**

130 All metal, Pb isotope, standard reference material, and analytical blank results are  
131 reported in the Supplementary Material (Tables S1, S2). Metal concentration ranges  
132 measured in honey from both the Île-de-France and Rhône-Alpes regions are comparable to  
133 those reported for other honey worldwide.<sup>23</sup> The levels of Pb measured in honey in this  
134 study (0.002-0.077 µg/g Pb in the Île-de-France and 0.002-0.009 µg/g Pb in the Rhône-

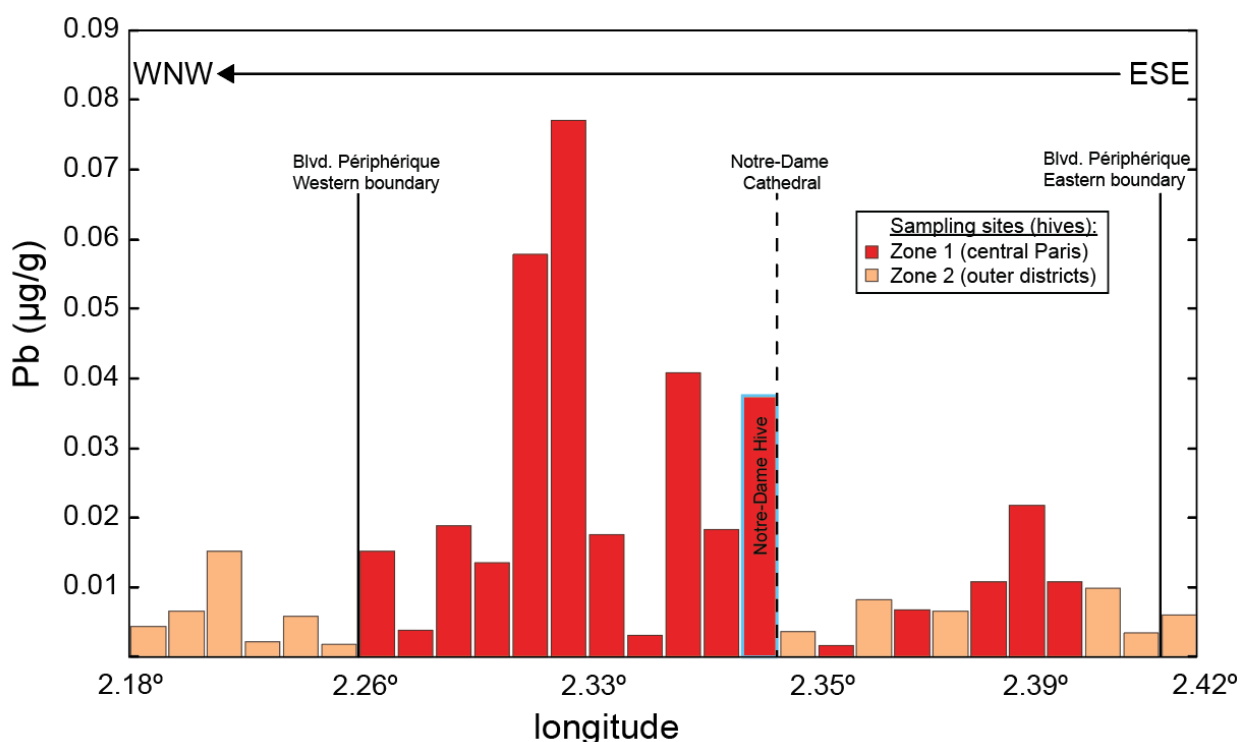
135 Alpes) are much lower than the range reported in French commercial honey by Devillers et  
136 al. (0.28-1.08  $\mu\text{g/g Pb}$ )<sup>24</sup>, and more comparable to values reported by Lambert et al. (0.004-  
137 0.378  $\mu\text{g/g}$ ), collected throughout Western France.<sup>25</sup> Our Pb results do not indicate any food  
138 safety concerns; they all meet EU regulation for maximum allowable Pb content ( $< 0.10$   
139  $\mu\text{g/g}$ ).<sup>26</sup> Ecologically, the concentrations measured in honeys in this study should not  
140 negatively affect bee health. In fact, maximum measured values of Pb (0.077  $\mu\text{g/g}$ ), Cd  
141 (0.007  $\mu\text{g/g}$ ), and Cu (1.14  $\mu\text{g/g}$ ) are well below the LC<sub>50</sub> (lethal concentration) thresholds  
142 calculated for honey bees (larvae and foragers) after Di et al.<sup>27</sup>:  $< 243 \mu\text{g/g Pb}$ ,  $< 0.19 \mu\text{g/g}$   
143 Cd,  $< 4.91 \mu\text{g/g Cu}$  (using 1.42 g/mL as average honey density<sup>28</sup>).

144 Concentrations of elements associated with human activity, high-density commercial  
145 and industrial land use, and pollution sources within a city (e.g. Ti, Cu, Zn, Ni, Pb, Sb) are  
146 generally elevated in honey from near the Paris city center (Fig. 1, S2, S3). Sources for these  
147 metals include urban runoff (e.g. from Zn rooftops), traffic emissions, vehicle and brake  
148 wear, industrial centers like railyards, and relatively recent legacy pollutants (i.e., leaded  
149 paint and gasoline from the twentieth century). These concentration trends are in  
150 agreement with previous studies that examined metal distribution patterns in Paris and the  
151 surrounding region using topsoil and aerosols<sup>29-31</sup> and in other urban areas (Vancouver,  
152 Canada and Sydney, Australia) using honey.<sup>11,12,14</sup>

153 The (geometric) mean Pb concentration measured in central Parisian (Fig. 1, 'Zone  
154 1') honey in 2019 (0.014  $\mu\text{g/g}$ ) is higher than the 2018 Parisian honey blend (0.009  $\mu\text{g/g}$ ) and  
155 higher than that of honey from the Rhône-Alpes (0.004  $\mu\text{g/g}$ ) (Fig. 3, inset). Overall, honey  
156 from central Paris, from 2018 and 2019, has higher Pb concentrations than the Rhône-Alpes  
157 honey (Fig. S3), but comparable amounts of other measured elements, indicating that the  
158 Pb levels in Parisian honey are a product of prolonged, concentrated human activity in a



159 large conurbation, of which the fire is included. Distinctly higher Pb concentrations are  
 160 present in honey collected west of the cathedral (downwind) (0.023  $\mu\text{g/g}$  mean Pb)  
 161 compared to other honey from central Paris (0.008  $\mu\text{g/g}$ ). The distribution of higher Pb  
 162 concentrations in honey corresponds to the areas where dust and topsoil with elevated Pb  
 163 concentrations (relative to the areas of central Paris outside of the plume range) were  
 164 discovered in the weeks following the fire<sup>21,32</sup> (Fig. 1, 2). This indicates that dust from the  
 165 fire likely contributed to Pb concentration trends in the 2019 honey.



166

167 **Fig. 2.** Lead concentration plot of all honey collected within Zones 1 and 2 (n = 28, each bar  
 168 represents one hive/honey sample), arranged by longitude and projected onto a vector  
 169 following the wind direction on 15 April 2019: right to left = east-southeast to west-  
 170 northwest (Fig 1). Note that the x-axis scale varies since some areas contain more hives than  
 171 others; longitude is approximate (to protect the privacy of the community members and  
 172 businesses that host the hives, we cannot disclose the hives' exact coordinate locations).  
 173

174

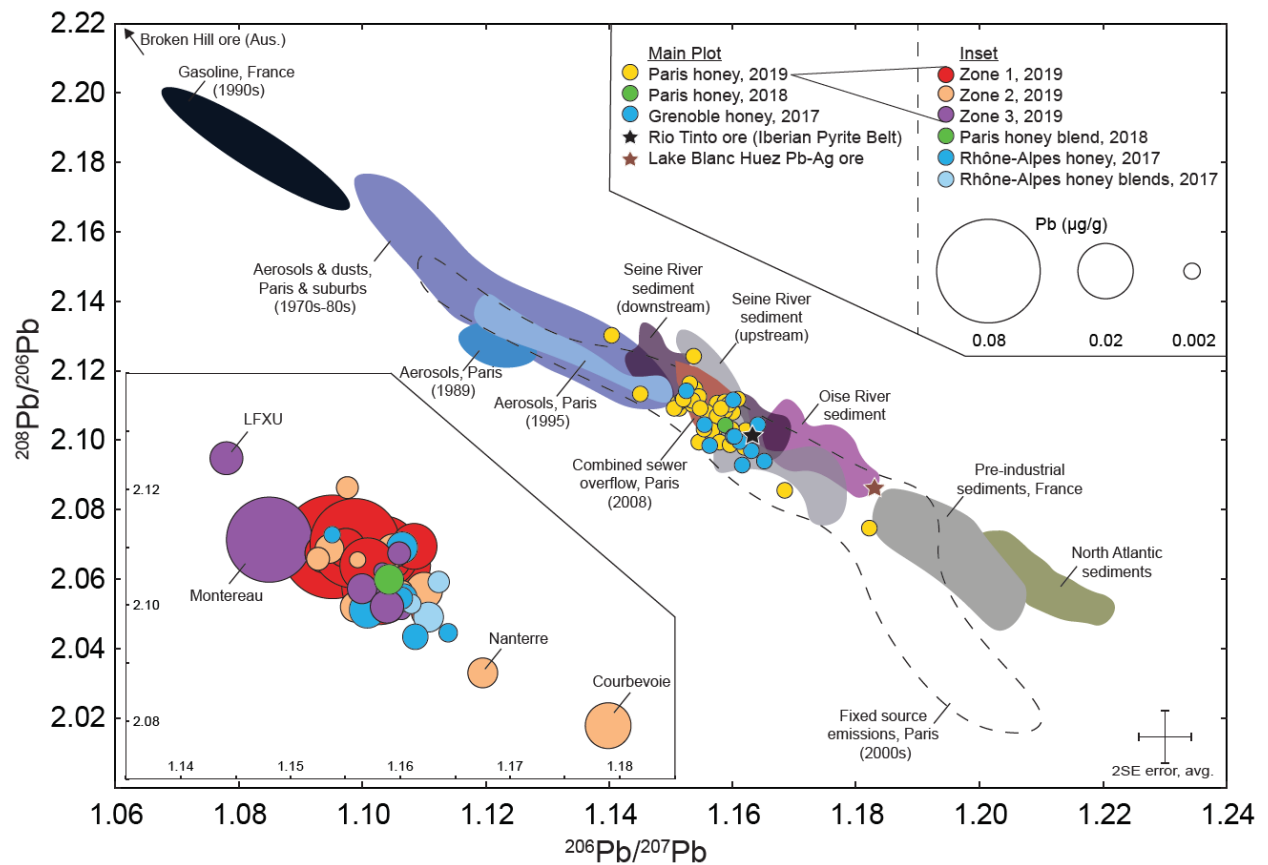
The 2019 Parisian honey has a  $^{206}\text{Pb}/^{207}\text{Pb}$  and  $^{208}\text{Pb}/^{206}\text{Pb}$  compositional range of

175

1.144-1.179 and 2.079-2.125, respectively, with a (geometric) mean composition of  $1.158 \pm$

176 0.004,  $2.106 \pm 0.006$  (all uncertainties reported as  $2 \times$  standard error of the geometric  
177 mean). The Pb isotopic composition of the pre-fire (2018) Parisian honey blend matches the  
178 2019 mean honey composition within error ( $1.159 \pm 0.003$ ,  $2.104 \pm 0.005$ ), and the isotopic  
179 range for the Rhône-Alpes honey ( $1.154$ - $1.164$  for  $^{206}\text{Pb}/^{207}\text{Pb}$  and  $2.095$ - $2.112$  for  
180  $^{208}\text{Pb}/^{206}\text{Pb}$ ) is more limited but falls within the Parisian range. While variation exists in the  
181 Pb isotopic composition of the Parisian honey, no strong geospatial trends are evident.  
182 However, some anomalous Pb isotopic compositions may be explained by nearby land use:  
183 for example, potential aviation gasoline use at the small airfield near Les Mureaux (some  
184 aviation fuels for small aircraft contain tetraethyl Pb) or railyard activity in  
185 Nanterre/Courbevoie (Fig. 1, 3). These findings contrast with previous studies that found  
186 predictable and reproducible differences between the Pb isotopic composition of rural and  
187 urban honey that was dependent on proximity to point sources within an urban area.<sup>11,12,14</sup>  
188 The key difference is that these studies were completed in much younger cities (Vancouver,  
189 Canada and Sydney, Australia), both of which have a much shorter history of Pb use,  
190 without the complex history of non-ferrous metal use prior to the Industrial Revolution in  
191 Europe: development of early cupellation (refining) techniques (Copper Age), use of Pb in  
192 alloys (Bronze Age), and then the rise and subsequent growth of the Roman Empire which  
193 helped spread Pb use throughout Europe.<sup>33</sup>

194



195

196 **Fig. 3. Main plot:** Lead isotope plot for all honey analyzed in this study, with some  
 197 anthropogenic and natural reference reservoirs, for context. Geologic/natural reference  
 198 reservoirs include North Atlantic sediment<sup>34</sup>, pre-industrial French sediments<sup>35</sup>, Lake Blanc  
 199 Blanc Huez ore<sup>36</sup>, Massif Central ore<sup>37</sup>, and Rio Tinto ore.<sup>38,39</sup> Industrial/anthropogenic reservoirs  
 200 include leaded gasolines used in France<sup>40</sup>, various aerosol emissions and dusts measured  
 201 throughout the twentieth century in France<sup>35,40-42</sup>, and sediments from the Seine and Oise  
 202 rivers.<sup>43</sup> ‘Fixed source emissions’ include emissions from boilers and waste incinerators  
 203 throughout Paris. The 2SE (2 × standard error) error bars denote average error for all honey  
 204 Pb isotope measurements in this study (n = 49). **Inset:** Pb isotope plot for all honey samples;  
 205 symbol size denotes Pb concentration. (See Fig. 1 for zone explanations.)  
 206

207

The history of France’s Pb use is reflected in Pb isotopic compositions of ores,  
 sediment records, gasoline and industrial emissions, and aerosols.<sup>e.g.,41,44</sup> Geologic

208

209 ‘background’ Pb in France has a  $^{206}\text{Pb}/^{207}\text{Pb}$  compositional range of 1.18-1.23 (e.g. Alpine Pb

210

deposits and pre-Roman lake sediment<sup>36,45</sup>). In Paris, the flux of materials (sources and

211

amounts) varied over the last two millennia, as needs and trade changed during

212

development, urbanization, industrialization, and subsequent de-industrialization of the île-

213 de-France region.<sup>2</sup> Historically, France has had few non-ferrous metal mines (e.g. Pb, Cu,  
214 Zn), so ores were imported from elsewhere in Western Europe (U.K., Germany, Belgium,  
215 Iberia), North Africa (Morocco), North America (U.S.A. and Mexico), and Australia.<sup>44</sup> North  
216 African and Western European sources of Pb ore have  $^{206}\text{Pb}/^{207}\text{Pb}$  compositions of 1.160-  
217 1.195, including the Rio Tinto ore from the Iberian Pyrite Belt which was likely a major  
218 source of Pb ore for the Île-de-France during the nineteenth century when the new spire  
219 was constructed at Notre-Dame cathedral.<sup>2,44</sup>

220           During the twentieth century, a major excursion in Pb isotopic compositions  
221 occurred in the Parisian environment (and in many other regions) due to the use of leaded  
222 gasoline.<sup>41,43</sup> Varying combinations of Pb sources were used to produce the tetraethyl Pb  
223 additive used in western Europe, but all formulations contained some amount of the Broken  
224 Hill ore (Australia), which is distinctly less radiogenic ( $^{206}\text{Pb}/^{207}\text{Pb} = 1.04$ ,  $^{208}\text{Pb}/^{206}\text{Pb} = 2.23$ )  
225 than other Pb ores used throughout France's history.<sup>41</sup> Lead isotopic compositions of  
226 environmental matrices have returned to more radiogenic compositions in the past decades  
227 (Fig. 3), driven by the phase-out of leaded gasoline and increased recycling of industrial Pb.<sup>2</sup>  
228 This isotopic shift has been observed in aerosols in western Europe<sup>46</sup>, aerosols in Paris and  
229 in France's northern industrial regions<sup>41</sup>, in sediments from the Seine (both upstream and  
230 downstream of Paris) and Oise Rivers<sup>43</sup>, and was accompanied by a decrease in Pb loadings  
231 in atmospheric total suspended particulates collected in Paris between 1994 and 2003.<sup>29</sup>  
232 Since the Pb isotopic compositions of the ores used throughout France during the  
233 nineteenth century (e.g., for building the new Notre-Dame spire in 1860) overlap with those  
234 of the modern Pb reservoir in France, the Pb from the fire did not measurably alter the  
235 isotopic composition of Parisian honey, despite an increase in concentrations in honey

236 downwind of the cathedral (Fig. 1, 2). This also explains why the Pb isotopic compositions of  
237 the Parisian honey overlap with those of honey collected elsewhere in France.

238 In summary, honey collected west (downwind) of the cathedral shows higher Pb  
239 concentrations resulting from the fire of Notre-Dame that generated an acute release of Pb  
240 into the environment. These findings complement the empirical results (and the modeled,  
241 interpolated Pb distribution) of a recent, post-fire topsoil survey in Paris.<sup>21</sup> Honey is, of  
242 course, no substitute for thorough public health assessments (e.g., indoor dust and blood Pb  
243 testing), whether performed routinely or immediately after an event like the Notre-Dame  
244 fire. Nonetheless, honey offers an accessible (hives are plentiful, sampling is low cost) and  
245 unique tool for visualizing urban metal distribution and this work serves as an interesting  
246 and timely case study for the application of honey as a biomonitor immediately following an  
247 acute Pb pollution event. While Pb isotopic compositions did not readily offer source  
248 apportionment leverage in this case (because of the overlap in Pb isotopic compositions  
249 among sources), the results are nonetheless supported by the history of Pb use in Paris.  
250 Future studies employing honey, especially in younger conurbations, are nonetheless likely  
251 to benefit from utilizing Pb isotopes.

## 252 **ASSOCIATED CONTENT**

253 Supporting Information:

254 Figures S1-S3

255 Tables S1-S2

256

## 257 **ACKNOWLEDGMENTS**

258 The authors thank the apiarists in the Île-de-France and Rhône-Alpes who contributed  
259 honey for this study and R. McMillan for manuscript editing and feedback. This work was  
260 funded by a Natural Sciences and Engineering Research Council of Canada (NSERC)  
261 Discovery Grant awarded to D. Weis. Funding for community outreach and networking  
262 opportunities (i.e., with Beeopic) was provided by the UBC Office of the Vice-President,

263 Research and Innovation (via the BeeHIVE Research Excellence Cluster). Additional funding  
264 for K. Smith was provided by UBC's International Doctoral Fellowship.

265

266 **Competing interests:** The authors declare no competing financial interests.

267

## 268 REFERENCES

- 269 (1) Casas, J. S.; Sordo, J. An Overview of the Historical Importance, Occurrence, Isolation,  
270 Properties and Applications of Lead. In *Lead*; Casas, J. S., Sordo, J., Eds.; Elsevier B.V.,  
271 2006; pp 1–40. <https://doi.org/10.1016/B978-044452945-9/50001-4>.
- 272 (2) Lestel, L. Non-Ferrous Metals (Pb, Cu, Zn) Needs and City Development: The Paris  
273 Example (1815-2009). *Reg. Environ. Chang.* **2012**, *12* (2), 311–323.  
274 <https://doi.org/10.1007/s10113-011-0255-4>.
- 275 (3) Hiatt, C. *Notre Dame de Paris, A Short History & Description of the Cathedral, with*  
276 *Some Account of the Churches Which Preceded It*; George Bell and Sons: London,  
277 1902.
- 278 (4) Deldicque, D.; Rouzaud, J.-N. Temperatures Reached by the Roof Structure of Notre-  
279 Dame de Paris in the Fire of April 15th 2019 Determined by Raman  
280 Paleothermometry. *Comptes Rendus Géoscience* **2020**, *352* (1), 7–18.
- 281 (5) Lesté-Lasserre, C. Saving Grace: Scientists Are Leading Notre Dame's Restoration-and  
282 Probing Mysteries Laid Bare by a Fire. *Science (80-. )*. **2020**, *367* (6483), 1182–1187.  
283 <https://doi.org/10.1097/01.NURSE.0000482875.55708.a4>.
- 284 (6) meteoblue. Climate Paris, Île-de-France Region, France <https://www.meteoblue.com/>  
285 (accessed May 1, 2020).
- 286 (7) de Campeau, A. Le Miel de Paris <https://www.lemieldeparis.com/> (accessed May 3,  
287 2020).
- 288 (8) Hladik, M. L.; Vandever, M.; Smalling, K. L. Exposure of Native Bees Foraging in an  
289 Agricultural Landscape to Current-Use Pesticides. *Sci. Total Environ.* **2016**, *542*, 469–  
290 477. <https://doi.org/10.1016/j.scitotenv.2015.10.077>.
- 291 (9) Gómez-Ramos, M. M.; García-Valcárcel, A. I.; Tadeo, J. L.; Fernández-Alba, A. R.;  
292 Hernando, M. D. Screening of Environmental Contaminants in Honey Bee Wax Comb  
293 Using Gas Chromatography–High-Resolution Time-of-Flight Mass Spectrometry.  
294 *Environ. Sci. Pollut. Res.* **2016**, *23* (5), 4609–4620. [https://doi.org/10.1007/s11356-](https://doi.org/10.1007/s11356-015-5667-0)  
295 [015-5667-0](https://doi.org/10.1007/s11356-015-5667-0).
- 296 (10) Sánchez-Hernández, L.; Hernández-Domínguez, D.; Martín, M. T.; Nozal, M. J.; Higes,  
297 M.; Bernal Yagüe, J. L. Residues of Neonicotinoids and Their Metabolites in Honey and  
298 Pollen from Sunflower and Maize Seed Dressing Crops. *J. Chromatogr. A* **2016**, *1428*,  
299 220–227. <https://doi.org/10.1016/j.chroma.2015.10.066>.
- 300 (11) Smith, K. E.; Weis, D.; Amini, M.; Shiel, A. E.; Lai, V. W.-M.; Gordon, K. Honey as a  
301 Biomonitor for a Changing World. *Nat. Sustain.* **2019**, *2* (3), 223–232.  
302 <https://doi.org/10.1038/s41893-019-0243-0>.
- 303 (12) Zhou, X.; Taylor, M. P.; Davies, P. J.; Prasad, S. Identifying Sources of Environmental  
304 Contamination in European Honey Bees (*Apis Mellifera*) Using Trace Elements and  
305 Lead Isotopic Compositions. *Environ. Sci. Technol.* **2018**, *52*, 991–1001.  
306 <https://doi.org/10.1021/acs.est.7b04084>.
- 307 (13) Taylor, M. P. Bees as Biomarkers. *Nat. Sustain.* **2019**, *2* (3), 169–170.  
308 <https://doi.org/10.1038/s41893-019-0247-9>.

- 309 (14) Smith, K. E.; Weis, D. Evaluating Spatiotemporal Resolution of Trace Element  
310 Concentrations and Pb Isotopic Compositions of Honeybees and Hive Products as  
311 Biomonitors for Urban Metal Distribution. *GeoHealth* **2020**, *4*.  
312 <https://doi.org/10.1029/2020GH000264>.
- 313 (15) Negri, I.; Mavris, C.; Di Prisco, G.; Caprio, E.; Pellecchia, M. Honey Bees (*Apis*  
314 *Mellifera*, L.) as Active Samplers of Airborne Particulate Matter. *PLoS One* **2015**, *10*  
315 (7), 1–22. <https://doi.org/10.1371/journal.pone.0132491>.
- 316 (16) Pellecchia, M.; Negri, I. Particulate Matter Collection by Honey Bees (*Apis Mellifera*,  
317 L.) near to a Cement Factory in Italy. *PeerJ* **2018**, *6*, e5322.  
318 <https://doi.org/10.7717/peerj.5322>.
- 319 (17) Komárek, M.; Ettler, V.; Chrástný, V.; Mihaljevič, M. Lead Isotopes in Environmental  
320 Sciences: A Review. *Environ. Int.* **2008**, *34* (4), 562–577.  
321 <https://doi.org/10.1016/j.envint.2007.10.005>.
- 322 (18) Shotyk, W.; Kempter, H.; Krachler, M.; Zaccone, C. Stable (206Pb, 207Pb, 208Pb) and  
323 Radioactive (210Pb) Lead Isotopes in 1year of Growth of Sphagnum Moss from Four  
324 Ombrotrophic Bogs in Southern Germany: Geochemical Significance and  
325 Environmental Implications. *Geochim. Cosmochim. Acta* **2015**, *163*, 101–125.  
326 <https://doi.org/10.1016/j.gca.2015.04.026>.
- 327 (19) Landrigan, P. J.; Fuller, R.; Acosta, N. J. R.; Adeyi, O.; Arnold, R.; Basu, N.; Baldé, A. B.;  
328 Bertollini, R.; Bose-O'Reilly, S.; Boufford, J. I.; et al. The Lancet Commission on  
329 Pollution and Health. *Lancet* **2018**, *391*, 462–512. [https://doi.org/10.1016/S0140-](https://doi.org/10.1016/S0140-6736(17)32345-0)  
330 [6736\(17\)32345-0](https://doi.org/10.1016/S0140-6736(17)32345-0).
- 331 (20) Mielke, H. W. Lead in New Orleans Soils: New Images of an Urban Environment.  
332 *Environ. Geochem. Health* **1994**, *16* (3–4), 123–128.  
333 <https://doi.org/10.1007/BF01747908>.
- 334 (21) van Geen, A.; Yao, Y.; Ellis, T.; Gelman, A. Fallout of Lead over Paris from the 2019  
335 Notre-Dame Cathedral Fire. *GeoHealth* **2020**, 1–16.  
336 <https://doi.org/10.1002/essoar.10503270.2>.
- 337 (22) Herrero-Latorre, C.; Barciela-García, J.; García-Martín, S.; Peña-Crecente, R. M. The  
338 Use of Honeybees and Honey as Environmental Bioindicators for Metals and  
339 Radionuclides: A Review. *Environ. Rev.* **2017**, *25* (4), 463–480.  
340 <https://doi.org/10.1139/er-2017-0029>.
- 341 (23) Solayman, M.; Islam, M. A.; Paul, S.; Ali, Y.; Khalil, M. I.; Alam, N.; Gan, S. H.  
342 Physicochemical Properties, Minerals, Trace Elements, and Heavy Metals in Honey of  
343 Different Origins: A Comprehensive Review. *Compr. Rev. Food Sci. Food Saf.* **2016**, *15*  
344 (1), 219–233. <https://doi.org/10.1111/1541-4337.12182>.
- 345 (24) Devillers, J.; Doré, J. C.; Marengo, M.; Poirier-Duchêne, F.; Galand, N.; Viel, C.  
346 Chemometrical Analysis of 18 Metallic and Nonmetallic Elements Found in Honeys  
347 Sold in France. *J. Agric. Food Chem.* **2002**, *50* (21), 5998–6007.  
348 <https://doi.org/10.1021/jf020497r>.
- 349 (25) Lambert, O.; Piroux, M.; Puyo, S.; Thorin, C.; Larhantec, M.; Delbac, F.; Pouliquen, H.  
350 Bees, Honey and Pollen as Sentinels for Lead Environmental Contamination. *Environ.*  
351 *Pollut.* **2012**, *170*, 254–259. <https://doi.org/10.1016/j.envpol.2012.07.012>.
- 352 (26) Commission Regulation (EU) 2015/1005 of 25 June 2015 Amending Regulation (EC)  
353 No 1881/2006 as Regards Maximum Levels of Lead in Certain Foodstuffs. *Off. J. Eur.*  
354 *Union* **2015**, *25* (L 161).
- 355 (27) Di, N.; Hladun, K. R.; Zhang, K.; Liu, T.-X.; Trumble, J. T. Laboratory Bioassays on the



- 356 Impact of Cadmium, Copper and Lead on the Development and Survival of Honeybee  
357 (*Apis Mellifera* L.) Larvae and Foragers. *Chemosphere* **2016**, *152*, 530–538.  
358 <https://doi.org/10.1016/j.chemosphere.2016.03.033>.
- 359 (28) Rybak-Chmielewska, H. Honey. In *Chemical and Functional Properties of Food*  
360 *Saccharides*; Tomasik, P., Ed.; CRC Press, Taylor & Francis Group: Boca Raton, 2003;  
361 pp 73–79.
- 362 (29) Ayrault, S.; Senhou, A.; Moskura, M.; Gaudry, A. Atmospheric Trace Element  
363 Concentrations in Total Suspended Particles near Paris, France. *Atmos. Environ.* **2010**,  
364 *44* (30), 3700–3707. <https://doi.org/10.1016/j.atmosenv.2010.06.035>.
- 365 (30) Saby, N.; Arrouays, D.; Boulonne, L.; Jolivet, C.; Pochot, A. Geostatistical Assessment  
366 of Pb in Soil around Paris, France. *Sci. Total Environ.* **2006**, *367* (1), 212–221.  
367 <https://doi.org/10.1016/j.scitotenv.2005.11.028>.
- 368 (31) Gaspéri, J.; Ayrault, S.; Moreau-Guigon, E.; Alliot, F.; Labadie, P.; Budzinski, H.;  
369 Blanchard, M.; Muresan, B.; Caupos, E.; Cladière, M.; et al. Contamination of Soils by  
370 Metals and Organic Micropollutants: Case Study of the Parisian Conurbation. *Environ.*  
371 *Sci. Pollut. Res.* **2018**, *25* (24), 23559–23573. [https://doi.org/10.1007/s11356-016-](https://doi.org/10.1007/s11356-016-8005-2)  
372 [8005-2](https://doi.org/10.1007/s11356-016-8005-2).
- 373 (32) Peltier, E.; Glanz, J.; Cai, W.; White, J. Notre-Dame’s Toxic Fallout. *The New York*  
374 *Times*. September 14, 2019.
- 375 (33) Shotyk, W.; Weiss, D.; Appleby, P. G.; Cheburkin, A. K.; Frei, R.; Gloor, M.; Kramers, J.  
376 D.; Reese, S.; Van der Knaap, W. O. History of Atmospheric Lead Deposition since  
377 12,370 14C Yr BP from a Peat Bog, Jura Mountains, Switzerland. *Science* (80-. ). **1998**,  
378 *281* (5383), 1635–1640.
- 379 (34) Sun, S. S. Lead Isotopic Study of Young Volcanic Rocks from Mid-Ocean Ridges , Ocean  
380 Islands and Island Arcs Author ( s ): S . -S . Sun Source : Philosophical Transactions of  
381 the Royal Society of London . Series A , Mathematical and Physical Sciences , Vol . 297  
382 , N. *Philos. Trans. R. Soc. London Ser. A, Math. Phys. Sci.* **1980**, *297* (1431), 409–445.
- 383 (35) Elbaz-Poulichet, F.; Holliger, P.; Martin, J. M.; Petit, D. Stable Lead Isotopes Ratios in  
384 Major French Rivers and Estuaries. *Sci. Total Environ.* **1986**, *54* (C), 61–76.  
385 [https://doi.org/10.1016/0048-9697\(86\)90256-1](https://doi.org/10.1016/0048-9697(86)90256-1).
- 386 (36) Garçon, M.; Chauvel, C.; Chapron, E.; Faïn, X.; Lin, M.; Campillo, S.; Bureau, S.;  
387 Desmet, M.; Bailly-Maître, M. C.; Charlet, L. Silver and Lead in High-Altitude Lake  
388 Sediments: Proxies for Climate Changes and Human Activities. *Appl. Geochemistry*  
389 **2012**, *27* (3), 760–773. <https://doi.org/10.1016/j.apgeochem.2011.12.010>.
- 390 (37) Baron, S.; Tămaş, C. G.; Rivoal, M.; Cauuet, B.; Télouk, P.; Albarède, F. Geochemistry  
391 of Gold Ores Mined During Celtic Times from the North-Western French Massif  
392 Central. *Sci. Rep.* **2019**, *9* (1). <https://doi.org/10.1038/s41598-019-54222-x>.
- 393 (38) Marcoux, E. Lead Isotope Systematics of the Giant Massive Sulphide Deposits in the  
394 Iberian Pyrite Belt. *Miner. Depos.* **1998**, *33*, 45–58.  
395 <https://doi.org/10.1007/s001260050132>.
- 396 (39) Pomiès, C.; Cocherie, A.; Guerrot, C.; Marcoux, E.; Lancelot, J. Assessment of the  
397 Precision and Accuracy of Lead-Isotope Ratios Measured by TIMS for Geochemical  
398 Applications: Example of Massive Sulphide Deposits (Rio Tinto, Spain). *Chem. Geol.*  
399 **1998**, *144* (1–2), 137–149. [https://doi.org/10.1016/S0009-2541\(97\)00127-7](https://doi.org/10.1016/S0009-2541(97)00127-7).
- 400 (40) Monna, F.; Lancelot, J.; Croudace, I. W.; Cundy, A. B.; Lewis, J. T. Pb Isotopic  
401 Composition of Airborne Particulate Material from France and the Southern United  
402 Kingdom: Implications for Pb Pollution Sources in Urban Areas. *Environ. Sci. Technol.*



- 403 **1997**, 31 (8), 2277–2286. <https://doi.org/10.1021/es960870+>.
- 404 (41) Véron, A.; Flament, P.; Bertho, M. L.; Alleman, L.; Flegat, R.; Hamelin, B. Isotopic  
405 Evidence of Pollutant Lead Sources in Northwestern France. *Atmos. Environ.* **1999**, 33  
406 (20), 3377–3388. [https://doi.org/10.1016/S1352-2310\(98\)00376-8](https://doi.org/10.1016/S1352-2310(98)00376-8).
- 407 (42) Widory, D.; Fiani, E.; Le Moullec, Y.; Gruson, S.; Gayraud, O. *Development of a Method*  
408 *for Characterising Contributions of Point Sources to Atmospheric Emissions of*  
409 *Particles Using a Multi-Isotopic Approach. Application to the Urban Area of Paris;*  
410 2004. <https://doi.org/10.3406/ridc.1989.1865>.
- 411 (43) Ayrault, S.; Le Pape, P.; Evrard, O.; Priadi, C. R.; Quantin, C.; Bonté, P.; Roy-Barman,  
412 M. Remanence of Lead Pollution in an Urban River System: A Multi-Scale Temporal  
413 and Spatial Study in the Seine River Basin, France. *Environ. Sci. Pollut. Res.* **2014**, 21  
414 (6), 4134–4148. <https://doi.org/10.1007/s11356-013-2240-6>.
- 415 (44) Ayrault, S.; Roy-Barman, M.; Le Cloarec, M. F.; Priadi, C. R.; Bonté, P.; Göpel, C. Lead  
416 Contamination of the Seine River, France: Geochemical Implications of a Historical  
417 Perspective. *Chemosphere* **2012**, 87 (8), 902–910.  
418 <https://doi.org/10.1016/j.chemosphere.2012.01.043>.
- 419 (45) Mariet, A. L.; Monna, F.; Gimbert, F.; Bégeot, C.; Cloquet, C.; Belle, S.; Millet, L.; Rius,  
420 D.; Walter-Simonnet, A. V. Tracking Past Mining Activity Using Trace Metals, Lead  
421 Isotopes and Compositional Data Analysis of a Sediment Core from Longemer Lake,  
422 Vosges Mountains, France. *J. Paleolimnol.* **2018**, 60 (3), 399–412.  
423 <https://doi.org/10.1007/s10933-018-0029-9>.
- 424 (46) Grousset, F. E.; Quétel, C. R.; Thomas, B.; Buat-Ménard, P.; Donard, O. F. X.; Bucher,  
425 A. Transient Pb Isotopic Signatures in the Western European Atmosphere. *Environ.*  
426 *Sci. Technol.* **1994**, 28 (9), 1605–1608. <https://doi.org/10.1021/es00058a011>.
- 427

Supplementary Materials for:

**Honey maps the Pb fallout from the 2019 fire at Notre-Dame Cathedral, Paris: a geochemical perspective**

Kate E. Smith\*, Dominique Weis\*, Catherine Chauvel, Sibyle Moulin

\*Correspondence to: [katesmith@eoas.ubc.ca](mailto:katesmith@eoas.ubc.ca), [dweis@eoas.ubc.ca](mailto:dweis@eoas.ubc.ca)

**This PDF file includes:**

Figs. S1 to S3

**Other Supplementary Materials for this manuscript include the following:**

Data: Tables S1 to S2

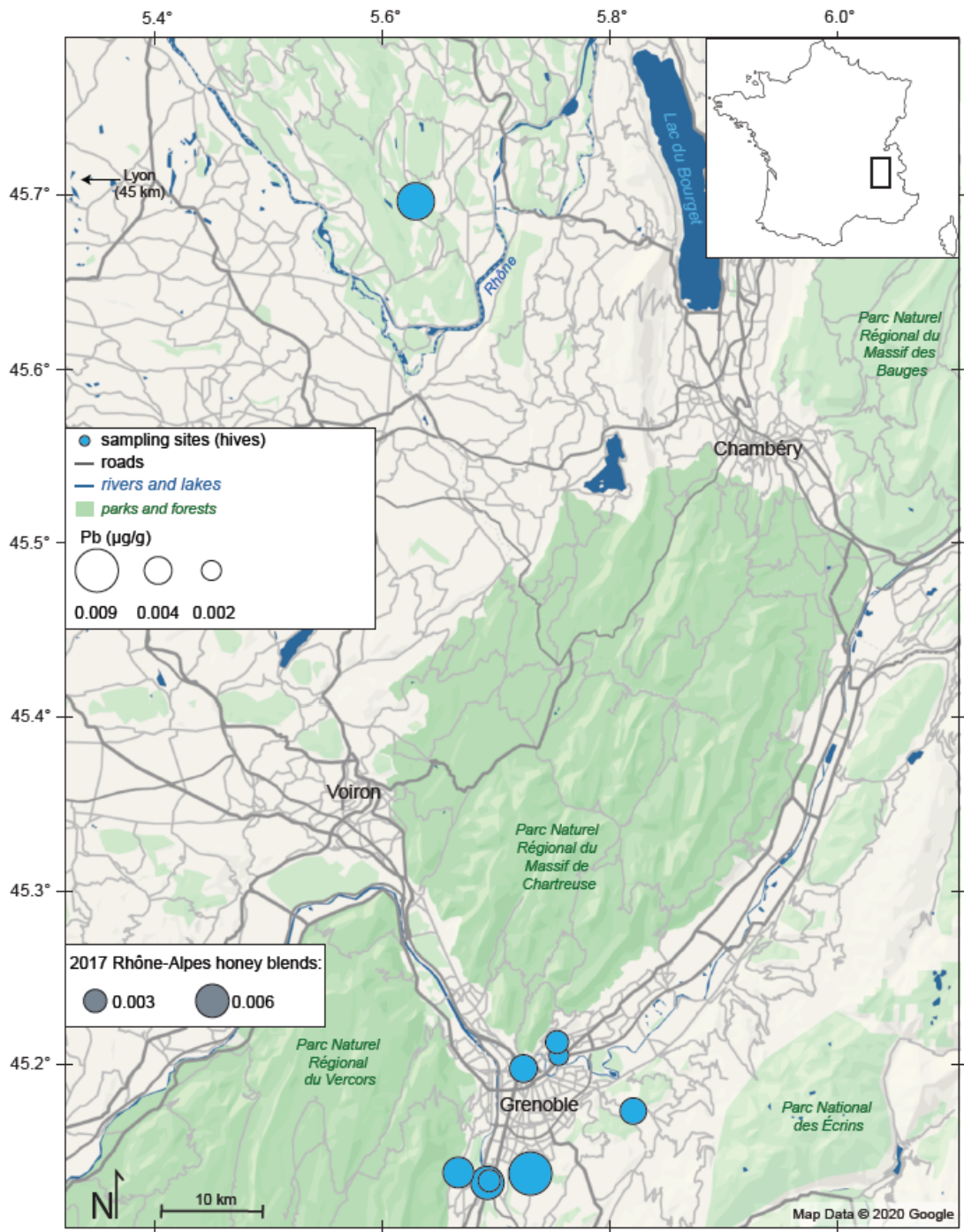


**Fig. S1.** Map of honey sampling sites in the Auvergne-Rhône-Alpes region. Symbol size denotes Pb concentration measured in the honey. Concentrations of local, commercial

honey blends are shown in an inset for comparison. All samples were collected or purchased in 2017.

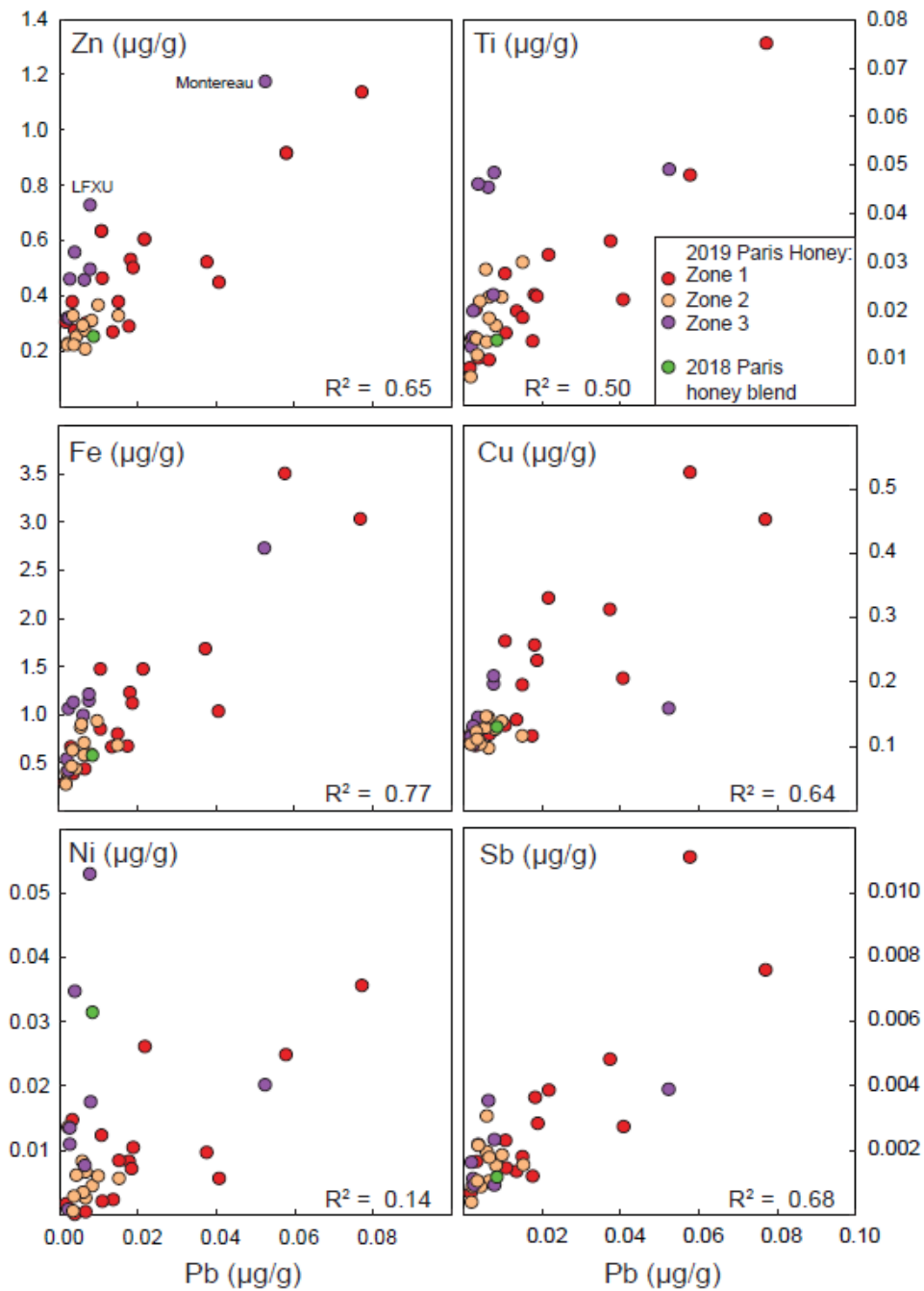


**Fig. S2.** Bivariate concentration plots for selected trace elements (versus Pb) for the Paris honey. All correlations are significant ( $p$ -value < 0.05). Symbol colors correspond to the sampling region/zone. (See Fig. 1 for zone explanations.)

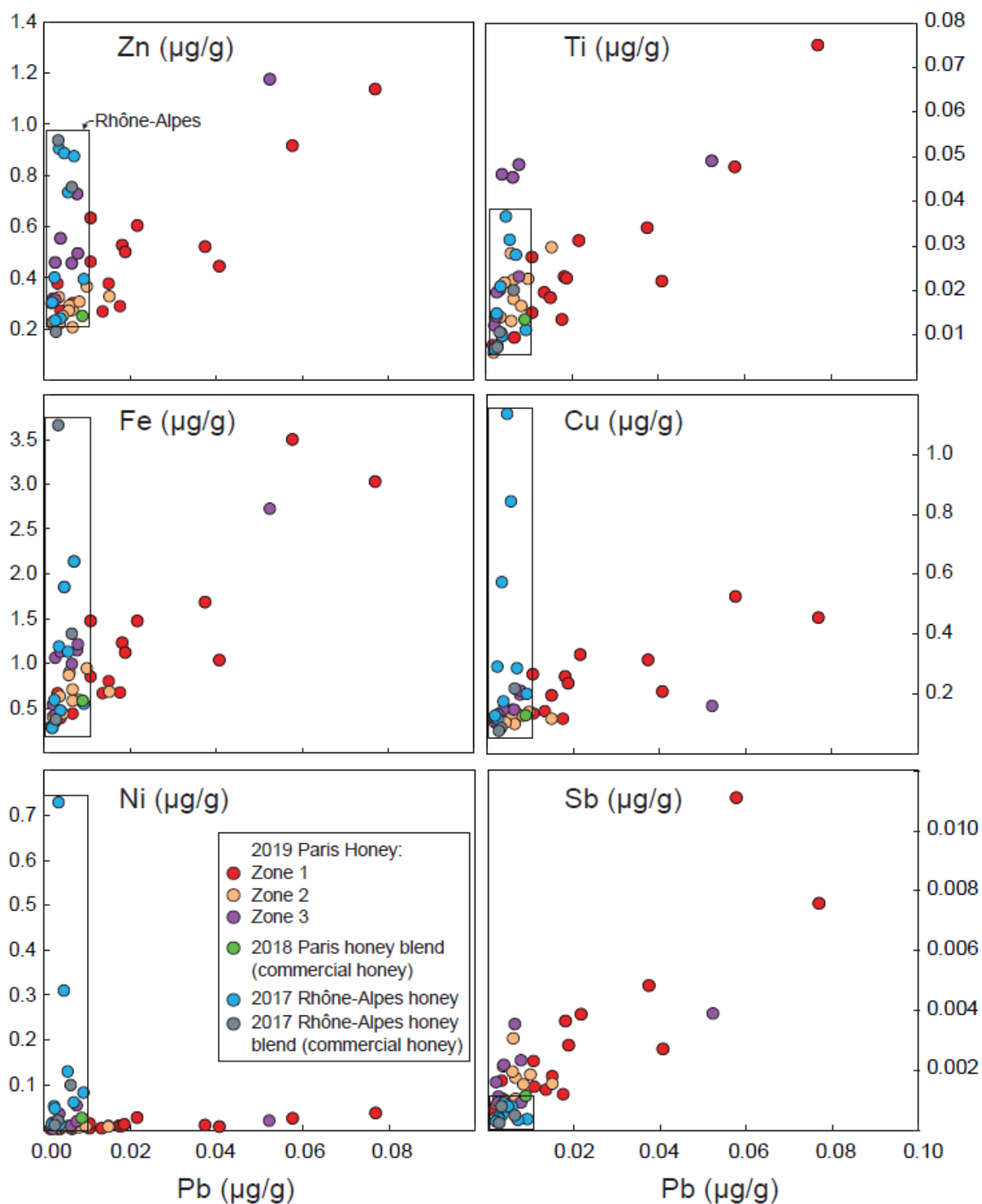


**Fig. S3.** Bivariate concentration plots for selected trace elements (versus Pb) for all honey included in this study (same as Figure S2 with the addition of the Rhône-Alpes honey). Symbol colors correspond to the sampling region/zone. (See Fig. 1 for Parisian zone explanations.)

**Supplemental Table 1. Honey Summary: Elemental concentrations and Pb isotopic co**

Sample name <sup>1</sup>	year produced	<sup>206</sup> Pb/ <sup>207</sup> Pb	2SE <sup>2</sup>
<b>Zone 1: City (within le Périphérique)</b>			
Paris 1	2019	1.158	0.003
Paris 2	2019	1.161	0.004
<b>Paris 4</b>	2019	1.158	0.003
Paris 5	2019	<b>1.155</b>	<b>0.007</b>
Paris 7	2019	1.155	0.003
Paris 8	2019	1.153	0.004
Paris 10	2019	1.159	0.004
Paris 11	2019	1.153	0.006
Paris 14	2019	1.155	0.007
Paris 15	2019	1.156	0.004
Paris 16	2019	1.161	0.003
Paris 17	2019	<b>1.157</b>	<b>0.002</b>
<b>Paris 19</b>	2019	1.157	0.005
<b>Paris 20</b>	2019	1.155	0.003
Paris 29	2019	1.154	0.003
Paris 30	2019	1.162	0.003
FranceMdP <sup>4</sup>	2018 <sup>7</sup>	1.159	0.003
<b>Zone 2: On or near le Périphérique</b>			
Paris 12	2019	1.155	0.004
Paris 13	2019	1.156	0.003
Paris 21	2019	1.156	0.006
Paris 22	2019	1.154	0.005
Paris 23	2019	1.153	0.004
Paris 18	2019	1.159	0.002
Paris 27	2019	1.162	0.005
Paris 31	2019	<b>1.158</b>	<b>0.004</b>
Paris 32	2019	1.168	0.003
Paris 33	2019	1.160	0.005
Paris 36	2019	1.179	0.002
Paris 39	2019	1.159	0.004
<b>Zone 3: Beyond the A86, away from Metro Paris</b>			
Paris 24	2019	1.144	0.003
Paris 26	2019	1.148	0.004
Paris 28	2019	1.158	0.005
Paris 34	2019	1.158	0.003
<b>Paris 35</b>	2019	1.157	0.004
Paris 37	2019	1.160	0.002
Paris 38	2019	1.159	0.004
Paris 40	2019	1.160	0.004
<b>Rhône-Alpes region honey</b>			
FranceMdFMaurecourtBlend <sup>5</sup>	2017 <sup>7</sup>	1.163	0.004
FranceMdFLesRdG <sup>6</sup>	2017 <sup>7</sup>	1.163	0.003
FranceMdLLesRdG <sup>6</sup>	2017 <sup>7</sup>	1.161	0.004
FranceOC17	2017	1.160	0.005

FranceBABG	2017	1.159	0.006
FranceFCoeur17	2017	1.157	0.003
FranceRIEUFJM17	2017	1.160	0.004
FranceRIEUFJVA17	2017	1.164	0.003
FranceRIEUFJP17	2017	1.161	0.006
FranceOM17	2017	1.156	0.002
FranceNatUG	2017	1.154	0.005
FrancePR17	2017	1.160	0.003

1. Bold, italic sample name is the average of two procedural duplicates; Bold results are

2. 2SE: 2 x standard error

3. All trace element concentration results are  $\mu\text{g/g}$

4. Miel de Paris-Commercial honey blend

5. Rhône-Alpes + non-E.U. honey blend, commercial

6. Rhône-Alpes honey blends, commercial

7. Production year is an estimate for commercial honeys

mpositions							
<sup>208</sup> Pb/ <sup>206</sup> Pb	2SE	<sup>207</sup> Pb/ <sup>206</sup> Pb	2SE	Pb <sup>3</sup>	%RSD	Mg	% RSD
2.103	0.007	0.863	0.002	0.0408	0.9	30.6	1.0
2.107	0.009	0.862	0.003	0.0176	0.9	33.5	1.2
2.109	0.008	0.863	0.002	0.0375	0.9	35.6	1.4
<b>2.112</b>	<b>0.009</b>	<b>0.866</b>	<b>0.005</b>	0.00165	1.5	19.1	1.1
2.114	0.008	0.866	0.002	0.0135	0.8	27.3	1.9
2.108	0.006	0.867	0.003	0.00380	1.1	16.3	2.0
2.107	0.003	0.862	0.003	0.00669	0.9	22.1	0.5
2.109	0.004	0.867	0.004	0.01078	0.4	18.3	2.0
2.11	0.012	0.866	0.005	0.0182	1.0	28.6	1.7
2.111	0.004	0.865	0.003	0.0578	0.9	42.1	1.1
2.110	0.007	0.861	0.002	0.0151	0.9	25.5	1.1
<b>2.107</b>	<b>0.005</b>	<b>0.864</b>	<b>0.002</b>	0.0188	1.2	29.5	2.0
2.107	0.008	0.864	0.004	<b>0.0217</b>	<b>0.7</b>	<b>42.7</b>	<b>1.8</b>
2.110	0.004	0.866	0.002	0.0107	0.9	21.6	0.8
2.110	0.004	0.867	0.002	0.0771	0.8	47.6	0.7
2.098	0.006	0.861	0.002	0.00318	1.6	18.3	0.9
2.104	0.005	0.863	0.003	0.0088	1.4	20.9	0.6
2.12	0.010	0.866	0.003	0.00339	0.9	23.6	1.7
2.100	0.007	0.865	0.002	0.00653	0.8	29.8	1.7
2.108	0.003	0.865	0.004	0.00188	1.7	16.5	1.3
2.110	0.005	0.867	0.004	0.00596	0.6	23.7	0.6
2.108	0.008	0.868	0.003	0.00368	1.9	17.6	1.3
2.109	0.004	0.863	0.002	0.0083	1.1	22.5	1.8
2.102	0.005	0.860	0.003	0.00987	0.4	21.7	1.2
<b>2.100</b>	<b>0.006</b>	<b>0.863</b>	<b>0.003</b>	0.00577	0.7	21.9	0.8
2.088	0.005	0.857	0.002	0.00653	0.8	18.13	0.3
2.103	0.003	0.862	0.004	0.00211	1.2	15.3	1.0
2.079	0.008	0.848	0.001	0.0151	0.8	26.0	0.7
2.108	0.005	0.863	0.003	0.00435	0.2	28.5	1.0
2.125	0.008	0.874	0.002	0.00774	0.4	44.8	0.6
2.111	0.007	0.871	0.003	0.0524	0.5	30.9	2.2
2.106	0.005	0.863	0.003	0.00204	0.9	18.8	1.1
2.102	0.003	0.864	0.002	0.00249	0.9	20.5	0.8
2.103	0.005	0.865	0.003	<b>0.00636</b>	<b>0.9</b>	<b>35.9</b>	<b>0.6</b>
2.109	0.004	0.862	0.002	0.00377	1.4	48.4	1.0
2.100	0.009	0.863	0.003	0.0078	1.2	41.0	0.8
2.099	0.006	0.862	0.003	0.00260	1.3	42.5	0.7
2.104	0.007	0.859	0.004	0.00331	1.1	19.7	0.7
2.098	0.002	0.860	0.003	0.00638	0.6	31.5	0.8
2.100	0.008	0.861	0.004	0.00272	1.9	5.98	0.7
2.101	0.009	0.862	0.005	0.00348	1.7	79.8	0.8



2.10	0.013	0.863	0.006	0.00382	1.7	26.2	1.0
2.099	0.007	0.864	0.003	0.0093	1.3	36	3.0
2.10	0.013	0.862	0.004	0.00554	0.7	73.8	0.9
2.095	0.008	0.859	0.003	0.00245	2.4	28.4	0.6
2.095	0.008	0.861	0.006	0.00474	1.0	67.4	1.0
2.10	0.010	0.865	0.002	0.00265	1.9	22.9	0.5
2.112	0.005	0.867	0.005	0.00195	0.8	23.1	1.0
2.110	0.006	0.862	0.003	0.00699	0.9	33.6	0.9

---

average of two analytical replicates (of the same digest) measured during the same analytical session, or two cc

Al	% RSD	Ti	% RSD	V	% RSD	Cr	% RSD	Mn
0.474	1.0	0.0220	1.4	0.00231	3.0	0.0037	5.1	0.265
0.455	0.7	0.013	9.4	0.00121	5.5	0.0016	6.2	5.15
0.83	1.6	0.034	3.5	0.0033	3.2	0.0064	5.3	0.78
0.099	2.3	0.008	14.9	0.00060	8.0	0.0008	16.1	0.0879
0.44	2.8	0.02	56.9	0.00135	1.7	0.0022	7.7	0.80
0.168	1.7	0.0098	6.0	0.00101	4.6	0.00146	6.3	0.207
0.214	1.4	0.009	14.5	0.00072	8.5	0.0017	7.6	0.244
0.482	1.6	0.015	17.7	0.00147	5.9	0.0028	7.3	0.402
0.514	0.7	0.023	8.1	0.00275	2.6	0.0048	3.4	0.287
1.180	0.6	0.048	2.8	0.0059	2.2	0.0158	2.7	0.477
0.417	1.8	0.0183	3.5	0.00188	2.8	0.0026	9.3	1.38
0.662	1.0	0.0226	2.3	0.00271	3.2	0.0061	7.9	0.447
<b>0.74</b>	<b>1.5</b>	<b>0.031</b>	<b>5.0</b>	<b>0.0034</b>	<b>3.5</b>	<b>0.0058</b>	<b>4.4</b>	<b>0.355</b>
0.618	1.1	0.027	4.5	0.00195	2.9	0.0043	6.9	0.412
1.83	0.7	0.0745	4.4	0.00504	1.2	0.0152	3.8	0.314
0.517	1.2	0.020	5.3	0.00148	4.0	0.0165	2.0	0.844
0.348	1.7	0.013	7.8	0.00113	3.5	0.0170	4.2	0.431
0.311	1.5	0.0139	6.2	0.00089	8.0	0.0016	6.9	0.555
0.50	2.3	0.0180	3.9	0.00169	4.0	0.00224	1.5	0.371
0.154	3.6	0.0060	7.3	0.00050	5.5	0.00029	10.4	0.558
0.369	0.8	0.0131	5.7	0.00134	6.8	0.0034	4.1	0.306
0.272	1.2	0.010	14.6	0.00124	5.5	0.0023	8.7	0.210
0.407	1.2	0.017	7.3	0.00157	4.3	0.0023	6.1	0.408
0.83	1.4	0.023	5.6	0.00229	4.1	0.0032	6.8	0.255
0.718	0.5	0.028	5.4	0.00201	2.5	0.0036	4.8	2.47
0.635	1.5	0.022	6.8	0.00152	3.4	0.0031	4.5	1.007
0.328	0.7	0.0139	6.6	0.00086	6.0	0.0018	15.2	2.023
0.648	0.9	0.030	4.0	0.00184	3.8	0.0064	7.2	0.514
0.415	0.7	0.022	4.8	0.00119	2.7	0.0019	6.1	1.023
1.188	0.7	0.023	8.4	0.0022	4.6	0.0030	8.7	22.9
1.68	1.5	0.0489	1.9	0.0038	3.1	0.042	2.6	0.570
0.384	0.4	0.012	10.4	0.00116	7.1	0.0026	9.9	0.195
0.448	0.7	0.020	14.3	0.00112	7.8	0.0015	10.7	0.495
<b>1.366</b>	<b>0.7</b>	<b>0.045</b>	<b>3.0</b>	<b>0.00360</b>	<b>1.8</b>	<b>0.0037</b>	<b>5.2</b>	<b>0.473</b>
1.37	0.9	0.046	2.3	0.00217	4.5	0.0036	2.8	15.65
1.189	0.7	0.048	3.6	0.00328	2.2	0.0045	2.7	2.42
0.325	0.7	0.0142	6.1	0.00082	3.8	0.0014	10.5	1.376
0.319	1.7	0.011	11.6	0.00150	4.2	0.0239	1.7	0.429
0.100	1.1	0.020	6.9	0.00164	4.5	0.0216	3.2	5.80
0.340	1.3	0.007	16.5	0.00083	9.9	0.0152	2.7	0.1226
14.4	1.0	0.021	9.4	0.00099	7.3	0.0028	7.6	4.06

0.343	1.8	0.0098	6.2	0.00064	6.9	0.0014	8.5	0.423
0.556	1.6	0.011	13.9	0.00084	4.7	0.0230	3.8	4.43
1.053	0.8	0.031	7.5	0.00226	3.6	0.0259	3.1	1.14
1.314	0.6	0.015	10.7	0.00109	4.8	0.0019	5.6	2.08
11.03	0.5	0.0365	1.6	0.00276	2.5	0.0072	6.6	2.01
0.162	2.6	0.008	14.1	0.00046	3.0	0.0203	2.3	0.95
0.123	2.1	0.007	14.6	0.00035	8.3	0.0012	8.6	0.574
1.35	0.7	0.028	6.5	0.00235	2.3	0.0182	2.7	0.551

---

onsecutive sessions

% RSD	Fe	% RSD	Co	% RSD	Ni	% RSD	Cu	% RSD
0.6	1.031	0.7	0.00107	3.2	0.0057	9.2	0.206	1.1
1.3	0.670	0.9	0.00120	2.4	0.0083	8.5	0.117	1.8
1.3	1.68	1.5	0.00154	4.0	0.0097	4.2	0.313	1.5
0.8	0.289	0.6	0.00035	7.3	0.0017	13.2	0.115	1.1
1.7	0.66	2.1	0.00064	4.4	0.002	46.9	0.141	2.0
2.1	0.383	2.1	0.00054	6.1	0.00010	46.2	0.111	2.0
1.2	0.434	0.6	0.00042	5.7	0.0005	148.0	0.119	1.2
1.5	0.85	1.5	0.0043	3.2	0.0021	40.9	0.133	1.6
1.5	1.22	1.7	0.00109	5.3	0.0071	6.0	0.258	1.8
1.3	3.50	1.3	0.00302	1.9	0.0248	3.4	0.526	1.9
1.1	0.792	0.5	0.00120	3.6	0.008	26.0	0.195	1.0
1.5	1.12	1.8	0.00173	3.6	0.010	13.0	0.233	1.5
<b>1.6</b>	<b>1.47</b>	<b>1.7</b>	<b>0.0028</b>	<b>2.6</b>	<b>0.0261</b>	<b>3.5</b>	<b>0.330</b>	<b>2.0</b>
0.5	1.47	0.9	0.00257	1.9	0.0123	0.8	0.264	1.1
0.6	3.03	0.8	0.00600	0.6	0.0356	1.0	0.453	1.4
0.9	0.664	1.0	0.00356	2.6	0.0148	3.5	0.101	1.3
0.5	0.578	0.3	0.00146	2.5	0.0307	1.6	0.1310	0.7
1.5	0.463	1.7	0.00051	4.9	0.0007	15.3	0.122	2.1
1.3	0.71	1.9	0.00092	1.8	0.0026	16.2	0.144	2.1
0.8	0.278	1.1	0.00076	4.6			0.103	1.3
0.8	0.899	0.7	0.00068	4.9	0.0035	7.1	0.146	1.3
1.1	0.63	1.8	0.00063	5.4	0.0028	29.9	0.111	1.3
1.8	0.59	1.7	0.00076	3.7	0.005	78.9	0.126	2.1
0.8	0.934	0.8	0.00119	2.7	0.006	36.0	0.139	1.2
0.7	0.861	0.9	0.00123	3.9	0.0084	1.7	0.129	1.1
0.8	0.579	0.6	0.00093	2.6	0.00671	1.0	0.0972	0.5
0.5	0.40	4.1	0.00114	2.9	0.0136	1.9	0.120	1.1
0.2	0.678	0.6	0.00075	3.1	0.0057	2.3	0.117	0.8
0.8	0.438	1.1	0.00063	4.3	0.0061	1.8	0.1038	0.8
1.0	1.142	0.4	0.00413	1.1	0.0529	1.8	0.197	1.2
0.5	2.72	0.7	0.00354	1.3	0.0202	3.7	0.159	1.2
1.5	0.533	1.0	0.00178	3.2	0.0009	72.7	0.114	1.4
0.3	1.054	0.6	0.00115	1.6	0.0110	1.9	0.1017	0.9
<b>0.3</b>	<b>0.990</b>	<b>0.3</b>	<b>0.00139</b>	<b>2.6</b>	<b>0.0077</b>	<b>2.5</b>	<b>0.1452</b>	<b>0.5</b>
0.5	1.128	0.5	0.00400	1.5	0.0346	0.9	0.145	0.8
0.4	1.205	0.2	0.00249	1.5	0.0176	1.7	0.210	0.5
0.6	0.414	1.1	0.00142	2.7	0.0135	1.6	0.131	0.9
0.6	3.65	1.1	0.00215	2.5	0.0195	1.4	0.0852	0.6
1.6	1.33	1.5	0.0051	2.1	0.098	1.3	0.2170	0.3
0.3	0.370	0.7	0.00069	2.0	0.0095	3.2	0.0766	0.4
0.9	1.18	1.1	0.0279	0.7	0.728	0.3	0.574	1.1

0.9	0.469	1.2	0.00067	2.7	0.0105	1.6	0.175	0.6
0.8	0.542	0.4	0.00282	2.8	0.0825	0.8	0.1986	0.5
1.7	1.128	0.7	0.00421	2.1	0.1281	0.7	0.844	0.8
1.2	0.584	0.8	0.00258	2.2	0.0518	0.5	0.2912	0.2
0.8	1.85	0.9	0.0171	0.7	0.308	0.4	1.135	0.7
1.3	0.340	0.5	0.00245	1.5	0.0469	1.1	0.1129	0.6
0.6	0.270	0.8	0.00117	1.1	0.0111	2.4	0.1251	0.4
0.4	2.14	1.2	0.0069	1.5	0.0590	0.6	0.284	0.4

---

Zn	% RSD	Ga	% RSD	As	% RSD	Rb	% RSD	Sr
0.445	0.9	0.0208	1.1	0.0017	9.2	3.33	1.2	1.22
0.288	1.4	0.0401	1.8	0.0009	17.5	4.41	1.6	2.35
0.520	1.1	0.0223	1.6	0.0021	9.1	3.10	1.3	1.03
0.301	0.4	0.0083	2.7	0.0007	27.8	2.37	0.6	0.576
0.267	1.7	0.0219	2.9	0.0013	20.5	2.99	1.4	2.26
0.271	2.1	0.0151	2.0	0.0004	32.9	1.82	2.1	0.370
0.300	0.8	0.0164	1.6	0.0005	29.3	2.83	0.9	2.01
0.462	1.7	0.0182	2.9	0.0017	7.1	2.15	1.3	0.798
0.53	2.3	0.0173	1.9	0.0013	8.2	2.66	1.3	0.63
0.91	1.3	0.0320	1.3	0.0024	14.4	2.26	1.3	0.421
0.376	1.2	0.0258	1.7	0.0014	18.7	2.64	1.2	0.615
0.501	1.2	0.046	3.0	0.0042	9.6	1.65	1.7	1.47
<b>0.60</b>	<b>2.1</b>	<b>0.0292</b>	<b>2.7</b>	<b>0.0017</b>	<b>8.4</b>	<b>1.95</b>	<b>1.6</b>	<b>1.94</b>
0.632	1.0	0.0117	2.6	0.0012	10.0	1.29	0.9	0.411
1.137	0.7	0.0258	1.0	0.0023	9.4	2.73	0.8	0.694
0.375	0.6	0.0112	2.4	0.0003	32.8	0.293	0.4	0.241
0.255	0.7	0.0180	1.2	0.0008	26.3	2.33	0.9	1.005
0.325	1.3	0.0215	2.2	0.0014	18.9	2.85	1.4	1.29
0.273	1.7	0.0235	1.6	0.0009	21.8	1.58	1.6	1.62
0.220	1.4	0.0332	1.1	0.00053	11.1	1.71	2.0	1.21
0.290	0.9	0.0207	1.8	0.0025	9.7	1.35	1.6	0.866
0.220	1.7	0.0092	1.2	0.00085	11.0	1.18	1.3	0.466
0.307	1.3	0.0234	3.1	0.0010	13.1	1.94	2.0	1.50
0.365	0.8	0.0309	2.2	0.0028	11.9	1.32	1.5	1.54
0.270	0.5	0.0272	1.8	0.0032	5.7	2.68	0.7	0.721
0.205	0.6	0.0253	1.3	0.0079	4.5	2.16	0.6	0.549
0.226	1.6	0.0183	1.3	0.00050	18.5	3.02	0.9	0.311
0.326	0.4	0.0254	0.8	0.0046	3.8	2.22	0.7	1.023
0.249	0.6	0.0296	0.7	0.0041	7.1	2.23	0.6	1.258
0.726	1.0	0.104	1.1	0.00136	6.2	11.8	0.9	0.362
1.17	0.9	0.0231	1.3	0.0021	12.5	0.580	0.6	0.108
0.318	1.0	0.0113	3.2	0.0005	22.7	0.88	1.3	0.276
0.316	0.6	0.0185	0.8	0.0004	25.9	0.647	0.6	0.497
<b>0.456</b>	<b>0.5</b>	<b>0.0149</b>	<b>1.5</b>	<b>0.0009</b>	<b>10.7</b>	<b>0.375</b>	<b>0.6</b>	<b>0.553</b>
0.555	0.7	0.0701	0.8	0.0010	14.6	5.78	0.4	0.272
0.494	0.6	0.0283	1.0	0.0015	8.8	1.493	0.4	0.2782
0.459	1.1	0.0202	0.7	0.00042	9.4	1.65	0.7	0.2636
0.937	0.2	0.0193	0.7	0.0042	7.9	0.341	0.5	0.1703
0.754	0.4	0.0516	1.5	0.0009	12.6	4.53	1.0	0.1308
0.187	0.7	0.0051	2.3	0.00033	17.4	0.174	0.7	0.0501
0.904	0.4	0.0334	1.7	0.0005	36.7	9.70	1.0	0.248

0.242	0.5	0.0168	1.0	0.00065	13.0	2.03	1.2	0.395
0.393	0.6	0.0560	0.7	0.0004	31.8	3.52	0.4	0.4095
0.734	0.4	0.0106	2.5	0.0009	25.5	5.83	0.8	0.1261
0.399	0.4	0.0277	0.6	0.0007	13.8	3.45	1.0	0.3337
0.887	0.4	0.0117	1.0	0.00102	7.2	9.92	0.8	0.0919
0.231	0.5	0.0223	2.1	0.0004	33.1	2.02	1.1	0.585
0.302	0.6	0.0312	1.6	0.00058	14.7	1.91	1.0	0.381
0.874	0.5	0.139	0.8	0.0012	8.4	0.669	0.4	0.670

---

% RSD	Zr	% RSD	Mo	% RSD	Cd	% RSD	Sn	% RSD
1.0	0.00224	2.9	0.0378	0.7	0.00026	21.8	0.00343	2.3
1.2	0.00114	4.4	0.0144	0.8	0.00026	9.4	0.00177	3.8
1.0	0.00405	1.7	0.0511	0.8	0.00039	16.1	0.0064	2.3
0.4	0.0014	10.4	0.00769	1.0	0.00005	34.8	0.00057	15.4
1.5	0.00252	3.0	0.0160	1.5	0.00018	22.7	0.00237	2.1
1.7	0.00081	2.5	0.00514	1.4	0.00007	33.6	0.00135	3.0
0.7	0.019	6.1	0.0139	1.8	0.00009	30.4	0.00097	6.5
1.1	0.0006	20.7	0.0099	1.6	0.00023	27.1	0.00037	8.6
1.8	0.0089	2.8	0.0350	0.4	0.00026	8.7	0.0053	3.2
1.0	0.0097	1.6	0.0599	0.9	0.00079	11.3	0.0232	3.2
0.7	0.0024	8.9	0.0194	2.2	0.00022	16.3	0.0036	3.0
1.9	0.0029	4.6	0.01257	0.5	0.00029	10.9	0.0059	2.3
<b>1.1</b>	<b>0.00380</b>	<b>2.3</b>	<b>0.0451</b>	<b>0.9</b>	<b>0.00066</b>	<b>4.9</b>	<b>0.0049</b>	<b>2.2</b>
0.5	0.0019	10.7	0.0127	0.9	0.00056	9.7	0.00339	2.1
0.7	0.0052	2.0	0.0290	1.1	0.0011	11.2	0.0138	1.1
0.5	0.00022	23.3	0.00391	1.5	0.00023	10.9	0.00054	5.2
0.7	0.00083	5.6	0.0185	1.2	0.00011	17.4	0.0207	1.3
1.8	0.00089	7.6	0.0138	1.5	0.00012	23.7	0.00075	3.0
1.7	0.00206	3.7	0.01891	0.4	0.00021	19.0	0.00161	2.8
1.3	0.00010	13.1	0.0148	1.1	0.00017	8.2	0.00030	19.9
0.6	0.022	6.8	0.0107	2.3	0.00017	22.4	0.00362	2.7
0.9	0.00269	3.1	0.0073	1.4	0.00009	26.1	0.0026	3.9
1.4	0.0029	3.6	0.0105	1.8	0.00013	28.9	0.00210	1.7
1.1	0.0024	6.4	0.0104	1.7	0.00015	31.1	0.00134	3.9
0.6	0.00066	5.5	0.0151	1.6	0.00026	11.8	0.00323	2.6
0.4	0.00031	12.5	0.0077	1.8	0.00023	6.2	0.00100	4.5
0.7	0.00122	2.5	0.0067	1.5	0.00022	12.4	0.00111	3.6
0.7	0.0021	9.2	0.0143	1.3	0.00014	12.9	0.00294	2.5
0.2	0.000026	9.5	0.0099	1.4	0.00018	7.2	0.00080	4.7
0.7	0.0049	6.5	0.00407	0.8	0.00083	10.9	0.00055	9.4
1.0	0.0156	1.9	0.00482	1.9	0.00109	4.6	0.00364	1.3
1.0	0.0010	15.8	0.0062	2.1	0.00015	35.0	0.000049	9.9
0.5			0.0095	1.4	0.00019	10.3	0.00051	5.8
<b>0.4</b>	<b>0.00084</b>	<b>11.5</b>	<b>0.00459</b>	<b>1.3</b>	<b>0.00021</b>	<b>16.7</b>	<b>0.00163</b>	<b>3.0</b>
0.5	0.0027	5.2	0.00289	1.8	0.00069	3.5	0.00190	5.0
0.2	0.00207	2.9	0.0180	0.6	0.00045	7.2	0.00210	2.4
0.3			0.00440	2.1	0.00026	17.6	0.00072	5.8
0.5	0.00116	4.5	0.0021	5.1	0.00012	16.0	0.0264	1.6
0.4	0.00095	2.3	0.0064	1.6	0.00062	5.4	0.0272	0.5
0.6	0.00141	3.8	0.00227	3.5	0.00005	21.5	0.0095	1.7
0.7	0.00054	12.8	0.0117	2.1	0.0037	2.8	0.00055	5.6



0.7	0.00158	4.7	0.0199	2.1	0.00015	15.9	0.00495	1.7
0.2	0.00044	3.5	0.0158	2.2	0.00030	12.5	0.00344	2.9
0.6	0.00069	5.2	0.0403	1.8	0.0015	10.2	0.0170	1.4
0.3	0.001	93.6	0.0144	2.1	0.0008	16.2	0.00699	1.1
0.3	0.0013	9.2	0.0326	1.6	0.0071	4.5	0.00902	0.8
0.4	0.00084	5.8	0.0153	1.9	0.00016	25.2	0.00239	2.6
0.4	0.00095	6.6	0.0212	1.3	0.00012	18.3	0.00023	4.2
0.3	0.00110	3.6	0.0060	1.7	0.00036	9.9	0.0281	0.8

---

Sb	% RSD	Ba	% RSD
0.00271	3.3	0.109	0.974687
0.00118	4.8	0.211	1.198142
0.00481	1.5	0.116	0.871506
0.00065	3.9	0.0430	1.001927
0.00133	3.4	0.115	1.822632
0.00100	2.5	0.079	1.728931
0.00097	2.5	0.086	1.447315
0.00144	4.8	0.093	2.058447
0.00363	1.9	0.089	1.365986
0.01110	0.9	0.162	1.346558
0.00178	2.6	0.134	0.813895
0.00282	1.1	0.237	1.334561
<b>0.00386</b>	<b>1.5</b>	<b>0.151</b>	<b>1.53558</b>
0.00230	1.5	0.0555	0.746658
0.00758	0.8	0.1280	0.607601
0.00163	0.8	0.0535	0.734999
0.00117	2.8	0.0829	0.5
0.00104	3.3	0.111	1.776254
0.00175	2.5	0.1200	0.511199
0.00037	3.3	0.170	1.740957
0.00305	1.6	0.107	0.964223
0.00213	1.1	0.046	2.117265
0.00151	2.0	0.121	2.216113
0.00183	1.3	0.156	0.941161
0.00195	1.2	0.133	0.827947
0.00102	4.3	0.125	0.942749
0.00084	3.9	0.0917	0.738285
0.00154	2.1	0.1285	0.569999
0.00086	3.5	0.1530	0.428368
0.00091	2.4	0.532	0.51187
0.00389	1.2	0.1066	0.657455
0.00160	1.3	0.0568	1.466535
0.00110	3.8	0.0929	0.508054
<b>0.00353</b>	<b>1.2</b>	<b>0.0733</b>	<b>1.172189</b>
0.00217	2.2	0.348	0.359006
0.00232	1.5	0.1402	0.46829
0.00091	2.8	0.1018	0.554794
0.00077	1.9	0.086	1.180141
0.00047	8.2	0.232	0.58504
0.00022	6.4	0.0216	2.126549
0.00050	4.2	0.162	1.107056

0.00089	5.2	0.0831	0.753278
0.00035	6.3	0.264	0.815053
0.00078	3.3	0.0512	1.680865
0.00041	5.8	0.1310	0.659435
0.00079	3.1	0.0593	1.181189
0.00034	9.2	0.108	1.231675
0.00027	6.5	0.157	0.689274
0.00031	5.0	0.610	0.368461

---

**Supplemental Table 2a. Pb Isotope Results and element concentrations<sup>1</sup> for**

Sample Name/Analysis Year	<sup>206</sup> Pb/ <sup>207</sup> Pb	2SE <sup>2</sup>	<sup>208</sup> Pb/ <sup>206</sup> Pb
SRM2018-1	1.214	0.003	2.025
SRM2018-2	1.210	0.003	2.032
SRM2018-3			
SRM2020-1	1.212	0.003	2.029
SRM2020-2	1.219	0.006	2.014
SRM2020-3	1.227	0.004	2.015
SRM2020-4	1.213	0.006	2.023
<b>Average</b>	1.216	0.004	2.023
<b>Standard Deviation</b>	0.006		0.007
<b>2SE (%), external precision</b>	4.2		2.9
<b>Certified or reference value<sup>4</sup></b>			

1. Instruments: Nu AttoM HR-ICPMS for Pb isotopes and Agilent 7700x ICP-MS

2. 2 x standard error

3. All concentration results and certified/reference values are in µg/g

4. Normal text: certified values, National Institute of Standards and Technology

Bold text: reference values, National Institute of Standards and Technology

Italicized text: values reported by Ertl & Goessler 2018 *Euro. Food Res. & Technol.*

**Supplemental Table 2b. Procedural Blanks<sup>1</sup> (pg)**

Sample/Date of Analysis	Mg	Al	Ti
23 Jan 2018-1	12618	8102	268
23 Jan 2018-2	11041	5728	84
9 Jan 2020-1	1838	1176	0
9 Jan 2020-2	8072	2885	51
27 Feb 2020-1	1993	1311	0
<b>Average, all blanks, n = 5</b>	7112	3840	81

1. Results reported as "0" were ≤ 0 after correcting for the matrix blank (2% HI)

Standard Reference Material NIST 1568b

2SE	<sup>207</sup> Pb/ <sup>206</sup> Pb	2SE	Pb <sup>3</sup>	%RSD	Mg	%RSD	Al
0.002	0.824	0.003	0.0114	1.2	494	1.9	3.88
0.003	0.827	0.003	0.01050	0.8	496	1.0	3.83
			0.01200	0.8	494	1.1	3.95
0.008	0.825	0.002	0.0115	1.6	494	0.9	3.88
0.006	0.821	0.004	0.0105	1.5	495	1.8	3.79
0.005	0.815	0.002	0.0120	1.1	517	0.5	4.53
0.007	0.824	0.004	0.0107	1.2	525	1.1	4.40
0.005	0.823	0.003	0.011	1.2	502	1.2	4.0
	0.004		0.001		13.1		0.30
	4.2		45		20		56
			<b>0.008</b>	<b>±0.003</b>	559	±10	4.21

S for trace element concentrations

8Y

1. 244:2065-2075.

V	Cr	Mn	Fe	Co	Ni	Cu	Zn
9	160	47	3877	8	174	55	1337
11	610	186	1403	44	1841	719	7380
0	29	5	460	2	0	0	290
0	713	52	1778	18	0	52	2058
10	110	17	1212	8	282	108	1363
6	324	61	1746	16	459	187	2486

NO<sub>3</sub>)

<b>%RSD</b>	<b>Ti</b>	<b>%RSD</b>	<b>V</b>	<b>%RSD</b>	<b>Cr</b>	<b>%RSD</b>	<b>Mn</b>	<b>%RSD</b>
1.6	0.180	5.1	0.0055	7.5	0.048	4.0	17.4	2.0
0.7	0.170	4.0	0.0059	4.3	0.024	6.1	17.2	1.2
1.3	0.19	9.3	0.0053	8.0	0.042	4.7	18.9	0.9
1.1	0.112	3.1	0.0056	4.7	0.025	5.3	18.3	0.9
2.1	0.101	4.0	0.0052	8.1	0.024	5.9	18.6	1.4
0.4	0.146	6.0	0.0059	4.0	0.060	3.4	18.6	0.9
1.1	0.124	5.1	0.0056	6.5	0.030	4.8	18.6	1.0
1.2	0.15	5.2	0.0056	6.1	0.04	4.9	18.2	1.2
	0.035		0.0003		0.014		0.66	
	181		37		296		27	
$\pm 0.34$			<i>0.005</i>	$\pm 0.001$	<i>0.0036</i>	$\pm 0.0010$	19.2	$\pm 1.8$

<b>Ga</b>	<b>As</b>	<b>Rb</b>	<b>Sr</b>	<b>Zr</b>	<b>Mo</b>	<b>Cd</b>	<b>Sn</b>	<b>Sb</b>
31	0	7	102	11	0	2	64	0
170	0	0	1288	109	0	7	26	0
10	0	0	32	138	100	0	191	6
72	0	0	195	116	101	2	160	10
12	0	0	30	264	65	2	0	1
59	0	1	329	128	53	3	88	3

Fe	%RSD	Co	%RSD	Ni	%RSD	Cu	%RSD	Zn
7.3	1.6	0.0205	1.1	0.212	1.5	1.981	0.3	16.6
5.84	1.0	0.0146	1.1	0.168	0.6	1.99	1.1	16.4
7.22	0.8	0.0164	1.6	0.195	1.2	2.06	0.6	17.2
7.02	1.0	0.0168	1.8	0.171	5.0	2.24	0.6	21.0
6.6	1.6	0.0161	1.9	0.19	6.3	2.28	2.0	22.3
7.25	0.9	0.0168	1.6	0.192	0.8	2.27	1.1	19.7
7.02	1.0	0.0163	1.3	0.181	1.2	2.28	0.9	19.7
6.9	1.1	0.017	1.5	0.19	2.4	2.2	0.9	19
0.52		0.002		0.015		0.14		2.3
57		81		61		49		91
7.42	±0.44	0.0177	±0.0005	0.20	± 0.06	2.35	±0.16	19.42

Ba	Pb
147	51
767	840
32	1
345	18
54	10
269	184

<b>%RSD</b>	<b>Ga</b>	<b>%RSD</b>	<b>As</b>	<b>%RSD</b>	<b>Rb</b>	<b>%RSD</b>	<b>Sr</b>	<b>%RSD</b>
1.8	0.0245	3.8	0.257	2.9	5.53	0.7	0.134	0.7
1.3	0.0242	1.3	0.265	2.6	5.42	1.5	0.128	1.2
0.7	0.025	4.4	0.268	1.9	5.70	0.9	0.133	0.9
1.3	0.0252	1.9	0.28	3.7	5.84	1.3	0.133	1.3
1.6	0.0249	3.4	0.285	2.5	6.0	2.3	0.134	1.8
0.7	0.0269	2.2	0.271	1.6	5.98	0.5	0.139	1.1
0.6	0.0255	1.9	0.273	2.2	5.93	0.3	0.135	1.4
1.1	0.0252	2.7	0.271	2.5	5.8	1.1	0.134	1.2
	0.0009		0.009		0.23		0.003	
	26		26		30		18	
$\pm 0.26$			0.285	$\pm 0.014$	6.198	$\pm 0.026$	0.12	$\pm 0.02$



Zr	%RSD	Mo	%RSD	Cd	%RSD	Sn	%RSD	Sb
0.0040	6.8	1.34	0.7	0.0190	4.0	0.0040	5.2	0.00041
0.0012	9.4	1.303	0.4	0.0189	3.8	0.0024	4.8	0.00043
0.0014	9.4	1.290	0.7	0.0186	4.2	0.0037	4.2	0.00038
0.0021	18.0	1.37	1.0	0.0215	2.6	0.0032	4.8	0.00012
0.0015	8.6	1.374	0.7	0.0206	2.4	0.0020	8.0	0.00032
0.0064	14.7	1.32	0.9	0.0199	4.7	0.0036	6.9	0.00110
0.0022	17.3	1.30	0.8	0.0203	2.7	0.0034	8.8	0.00036
0.003	12.0	1.33	0.7	0.020	3.5	0.0032	6.1	0.0004
0.002		0.03		0.001		0.0007		0.0003
531		19		40		172		520
		1.451	±0.048	0.0224	±0.0013	<b>0.005</b>	<b>±0.001</b>	<i>&lt;0.001</i>

<b>%RSD</b>	<b>Ba</b>	<b>%RSD</b>
12.7	0.116	1.5
9.8	0.111	1.4
10.5	0.112	2.0
12.0	0.121	2.4
10.8	0.120	1.8
5.6	0.130	2.5
9.6	0.122	2.0
10.2	0.119	2.0
	0.007	
	42	
	<i>0.12</i>	<i>± 0.01</i>